https://doi.org/10.5194/acp-2020-152
Preprint. Discussion started: 7 May 2020

Atmospheric Chemistry and Physics Discussions

Measurement Report: important contributions of oxygenated compounds to emissions and chemistry of VOCs in urban air

Caihong Wu[1,2,#], Chaomin Wang[1,2,#], Sihang Wang[1,2], Wenjie Wang[3], Bin Yuan[1,2,*], Jipeng Qi[1,2], Baolin Wang[5], Hongli Wang[6], Chen Wang[5], Wei Song[4], Xinming Wang[4], Weiwei Hu[4], Shengrong Lou[6], Chenshuo Ye[3], Yuwen Peng[1,2], Zelong Wang[1,2], Yibo Huangfu[1,2], Yan Xie[7], Manni Zhu[7], Junyu Zheng[1,2], Xuemei Wang[1,2], Jiang Bin[1,2], Zhanyi Zhang[1,2], Min Shao[1,2,*]

[1] Institute for Environmental and Climate Research, Jinan University, Guangzhou 511443, China.
[2] Guangdong-Hongkong-Macau Joint Laboratory of Collaborative Innovation for Environmental Quality, Guangzhou 511443, China.
[3] State Joint Key Laboratory of Environmental Simulation and Pollution Control, College of Environmental Sciences and Engineering, Peking University, Beijing 100871, China
[4] The State Key Laboratory of Organic Geochemistry, Guangzhou Institute of Geochemistry, Chinese Academy of Sciences, Guangzhou 510640, China
[5] School of Environmental Science and Engineering, Qilu University of Technology，Jinan 250353, China
[6] State Environmental Protection Key Laboratory of Formation and Prevention of Urban Air Pollution Complex, Shanghai Academy of Environmental Sciences, Shanghai 200233, China
[7]College of Environment and Energy, South China University of Technology, Guangzhou 510006, China.

#C.H.W. and C.M.W. contributed equally to this work.

*Correspondence to: byuan@jnu.edu.cn; mshao@pku.edu.cn

https://doi.org/10.5194/acp-2020-152
Preprint. Discussion started: 7 May 2020

Atmospheric Chemistry and Physics Discussions

Abstract:

Volatile organic compounds (VOCs) play important roles in the tropospheric atmosphere. In this study, VOCs were measured at an urban site in Guangzhou, one of the mega-cities in Pearl River Delta (PRD) using a gas chromatograph mass spectrometer/flame ionization detection (GC-MS/FID) and a proton transfer reaction time-of-flight mass spectrometer (PTR-ToF-MS). Diurnal profile analyses show that stronger chemical removal by OH radicals for more reactive hydrocarbons during the daytime. Diurnal profiles of OVOCs indicate evidence of contributions from secondary formation. Detailed source analyses of OVOCs using a photochemical age-based parameterization method suggest important contributions from both primary emissions and secondary formation for measured OVOCs. During the campaign, around 1700 ions were detected in PTR-ToF-MS mass spectra, among of which 462 ions with noticeable concentrations. VOCs signals from these ions without calibration in PTR-ToF-MS are quantified based on sensitivities of available VOCs species. OVOC-related ions dominated PTR-ToF-MS mass spectra with an average contribution of 77.2%. Combining measurements from PTR-ToF-MS and GC-MS/FID, OVOCs contribute 57.4% to the total concentration of VOCs. Using concurrent measurement of OH reactivity, OVOCs measured by PTR-ToF-MS contribute greatly to the OH reactivity (19.3%). In comparison, hydrocarbons account for 20.0% of OH reactivity. Adding up the contributions from inorganic gases (47.9%), ~12% of the OH reactivity remains as "missing". Our results demonstrate the important roles of OVOCs in the emission and evolution budget of VOCs in urban atmosphere.

https://doi.org/10.5194/acp-2020-152
Preprint. Discussion started: 7 May 2020


Atmospheric Chemistry and Physics Discussions

1. Introduction

Volatile organic compounds (VOCs) play important roles in the tropospheric atmosphere. The oxidation of VOCs by various oxidants contribute to the formation of ground-level ozone (O_3) and secondary organic aerosols (SOA) (Louie et al., 2013;Ran et al., 2011), influencing both regional air quality and climate change (Fry et al., 2013). Some selected VOCs (e.g. benzene and formaldehyde) are harmful to human health, especially in urban environments (Simpson et al., 2013).

Oxygenated volatile organic compounds (OVOCs) are an important group of VOCs. OVOCs mainly consist of aldehydes and ketones, low molecular organic acids and organic alcohols. The sources of OVOCs in the environment are complicated. They can be emitted from primary anthropogenic emissions such as vehicle exhaust (Gentner et al., 2013), biomass burning (Gilman et al., 2015) and industries (Kim et al., 2008), and also can be formed by the photo-oxidation of other VOCs in the atmosphere (Millet et al., 2015). Besides anthropogenic sources, biogenic emissions are reported to contribute significantly to many OVOCs species (Park et al., 2013). The oxidation of OVOCs by various oxidants and their direct photolysis can have an important effect on the radical budget and formations of secondary pollutants in the atmosphere (Mellouki et al., 2015).

The total OH reactivity can intuitively and effectively characterize the contributions of various VOCs to atmospheric chemical reaction, especially the generation of secondary pollutants (Yang et al., 2016). OVOCs has been reported as a large contributor to the total OH reactivity in a variety of environments (Gilman et al., 2013;Pfannerstill et al., 2019). Aldehydes and other OVOCs were found to contribute 30-50% of modeled urban VOC reactivity (up to 30 s^{-1}) (Lou et al., 2010). In large cities, OVOCs contributed between 11-24% of OH reactivity (Mao et al., 2010;Kim et al., 2016). Even though there has been a great number of studies focusing on the OH reactivity measurements, substantial differences between measured and calculated or modeled OH reactivity, termed as “missing” reactivity, were revealed in many field campaigns (Dolgorouky et al., 2012;Hansen et al., 2014;Praplan et al., 2017).

https://doi.org/10.5194/acp-2020-152
Preprint. Discussion started: 7 May 2020


Atmospheric Chemistry and Physics Discussions

Unmeasured primary and secondary organic species produced by photochemical oxidation in the atmosphere likely contributed to the missing reactivity (Karl et al., 2009;Wolfe et al., 2011;Ferracci et al., 2018). The unmeasured OVOC species are proved to contribute large fractions to the missing reactivity based on previous observation studies (Kim et al., 2016) and model simulation (Lou et al., 2010;Whalley et al., 2016).

Proton-transfer-reaction mass spectrometry (PTR-MS) has been demonstrated to effectively detect many VOCs in the atmosphere with fast response and high sensitivity (Yuan et al., 2017;de Gouw and Warneke, 2007). The applications of time-of-flight mass spectrometry (TOF-MS) in PTR-MS in recent years provide significantly higher mass resolution and measurements of the whole mass spectra (Yuan et al., 2017), which offered the opportunity to quantify much more VOC species in the atmosphere (Cappellin et al., 2012), especially numerous oxygenated VOCs species. However, it is unrealistic to experimentally calibrate all of the VOC species (hundreds to thousands) detected in the atmosphere. Moreover, gas standards are not commercially available or easy to make in the laboratory. Several parameterization methods have been established to estimate calibration factors of the uncalibrated species measured by PTR-ToF-MS, which facilitates the investigation of these compounds in different environments (Stockwell et al., 2015;Sekimoto et al., 2017;Koss et al., 2018;Holzinger et al., 2019). However, to the best of our knowledge, there is no attempt to conduct such analysis in urban air to better evaluate the roles of these oxygenated species.

In this study, we conducted intensive observations of VOCs concentrations and the total OH reactivity at an urban site in southern China. We performed systematic analysis on diurnal profiles to investigate photochemical losses of various hydrocarbons and secondary formation of OVOCs. After considering VOC signals from uncalibrated species in PTR-ToF-MS, we used the combined dataset to analyze contributions of different VOCs groups to total VOCs concentrations. A photochemical age-based parameterization method was applied to quantify the contributions from different atmospheric processes to concentrations of OVOCs. In the end, we evaluate the contributions of measured VOCs by both conventional methods and newly-quantified

https://doi.org/10.5194/acp-2020-152
Preprint. Discussion started: 7 May 2020


Atmospheric Chemistry and Physics Discussions

106 species from PTR-ToF-MS to OH reactivity in this region.

107 2. Experimental

108 Field measurements were conducted at an observation site in Guangzhou (113.2ºE,
109 23ºN) from September to November 2018. The sampling site (~25 m above the ground
110 level) is located on the 9th floor of a building on the campus of Guangzhou Institute of
111 Geochemistry, Chinese Academy of Sciences, which is regarded as a typical urban site
112 in Guangzhou.

113 2.1 VOC measurements using PTR-ToF-MS

114 During the campaign, a commercial PTR-QiToF-MS (Ionicon Analytic GmbH,
115 Innsbruck, Austria) with H_3O^+ chemistry and NO^+ chemistry was used to measure
116 VOCs in the atmosphere. Ambient air was continuously introduced through an 8 m long
117 Teflon tubing (1/4") into PTR-ToF-MS with an external pump (5.0 L/min). The Teflon
118 tubing was wrapped with a self-controlled heater wire (40 °C) to prevent air
119 condensation inside the tubing. During the campaign, the PTR-ToF-MS automatically
120 switched between H_3O^+ and NO^+ chemistry every 10-20 minutes. In each ionization
121 mode, background measurements were automatically performed by passing ambient air
122 through a custom-built Platinum catalytical converter heated to 365 °C for 3 minutes.
123 The mass spectra of PTR-ToF-MS was recorded every 10 s.

124 When the PTR-ToF-MS was running at the H_3O^+ ionization mode, the drift tube
125 was operated at a pressure of 3.8 mbar, a temperature of 50 °C and a voltage of 920 V,
126 resulting in an operating E/N (E is the electric field and N is the number density of the
127 gas in drift tube) ratio of ~120 Td. At this condition, the fractions of water-cluster ions
128 are small, and the fragmentation of most VOCs product ions is not significant (de Gouw
129 and Warneke, 2007;Yuan et al., 2017). In this study, VOCs measured by H_3O^+ chemistry
130 will be shown. The additional species measured by NO^+ chemistry are discussed in a
131 companion paper (Wang et al., 2020). Higher alkanes measured by NO^+ chemistry will
132 be used in section 3.4 for OH reactivity calculation.

133 A 16-component VOC gas standard (Apel Riemer Environmental Inc.) was used
134 for daily calibrations under both dry (RH<1%) and ambient humidity during the

https://doi.org/10.5194/acp-2020-152
Preprint. Discussion started: 7 May 2020


Atmospheric Chemistry and Physics Discussions

campaign. As shown in Figure S3, the obtained VOCs sensitivities from automatical calibrations indicate quite stable instrumental performance during the campaign. Additional VOC gas standard with 23-component (Linde Spectra Environment Gases) was used during the later period of this campaign. Some additional VOCs species, including organic acids and nitrogen-containing species, were calibrated in the laboratory using a Liquid Calibration Unit (LCU, Ionicon Analytik). The sensitivities of the calibrated species are listed in Table S1. Humidity dependencies of various VOCs were determined in the laboratory with absolute humidity in the range of 0-30 mmol/mol (relative humidity of 0%-92% at 25 °C), which fully cover the humidity range encountered during the entire campaign. Figure S4 shows the humidity dependence of selected VOCs (benzene, toluene, C8 aromatics, formaldehyde, acetaldehyde and acetone) determined from laboratory experiments. We only observed significant humidity dependence for a few selected VOCs species, including formaldehyde, benzene, methanol, ethanol and furan, consistent with the results determined from other PTR-QiToF-MS instruments or similar quadrupole interfaced PTR-ToF-MS (Yuan et al., 2017;Koss et al., 2018;Kari et al., 2018). Humidity effects were taken into account during the calculation of concentrations for these VOCs species.

2.2 Other Measurements

A total of 56 non-methane hydrocarbons (NMHCs) were measured using a gas chromatography-mass spectrometer/flame ionization detector (GC-MS/FID) system, coupled with a cryogen-free pre-concentration device (Wang et al., 2014b). The system contains a two-channel sampling and GC column separation, able to measure C2-C5 hydrocarbons with the FID detection in one channel and measure C5-C12 hydrocarbons using MS detection in the other channel. In addition to PTR-ToF-MS, formaldehyde was also measured by a custom-built online instrument based on the Hantzsch reaction and absorption photometry from October 16 to November 20, 2018.

Inter-comparisons between different instruments for overlapped VOCs species were carefully evaluated. Good agreements for toluene, styrene, C8 aromatics, C9 aromatics between PTR-ToF-MS and GC-MS/FID are obtained during the campaign

https://doi.org/10.5194/acp-2020-152
Preprint. Discussion started: 7 May 2020


Atmospheric Chemistry and Physics Discussions

(Figure S5). Formaldehyde measured by PTR-ToF-MS shows reasonable agreement with the Hantzsch formaldehyde instrument.

Total OH reactivity was measured by the comparative reactivity method (CRM) (Sinha et al., 2008). The CRM system consists of three major components: an inlet and calibration system, a reactor and a measuring system. Here, pyrrole (C_4H_5N) was used as the reference substance in CRM and was quantified by a quadrupole PTR-MS (Ionicon Analytic, Austria). The calibration of the CRM system was conducted using single-species gas standard with propane and propene, respectively (Huayuan Gas Ltd, China). Measured and calculated OH reactivity agreed well within the uncertainty for all calibrations. The OH reactivity measurement by CRM method is interfered by high concentrations of ambient NO, which produces additional OH radicals via the recycling of HO_2 radicals (Sinha et al., 2008;Dolgorouky et al., 2012;Michoud et al., 2015). A series of experiments were conducted in the field to quantify the interference from NO, by introducing different levels of NO (0-100 ppb) and given amounts of VOC gas standard into the CRM reactor. A correction curve was derived from these NO-interference experiments and was used to correct the obtained OH reactivity according to simultaneously measured ambient NO concentrations. The detection limits of CRM methods in this campaign were around 5 s^{-1} and the total uncertainty was estimated to be about 20%.

Air-quality-related trace gases (including O_3, NO, NO_2, NO_x, CO, SO_2 and CH_4), together with meteorological data (i.e., temperature, solar radiation, precipitation, relative humidity, wind speed and wind direction) were also continuously measured in this campaign. Photolysis frequencies of H_2O_2、HCHO、HONO、NO_2、NO_3 and O^1D were obtained from measurements of a PFS-100 Photolysis spectrometer (Focused Photonics Inc.).

3 Results and discussion

3.1 Characteristics of selected VOCs

Diurnal variations of selected VOCs species measured by PTR-ToF-MS are shown in Figure 1. The time stamps are the middle time of the respective hourly data bin (e.g.

https://doi.org/10.5194/acp-2020-152
Preprint. Discussion started: 7 May 2020


Atmospheric Chemistry and Physics Discussions

10 for data averaged between 9:30 and 10:30).

Diurnal variations of hydrocarbons are controlled by multiple atmospheric processes, including variability of primary emissions, chemical removal by reactions with oxidants (e.g. OH radical, O_3 and NO_3) and boundary layer variations (de Gouw et al., 2017). As an abundant aromatic species, toluene had an average concentration of 1.8±1.9 ppb during the campaign. Toluene concentrations varied little throughout the day with lower concentrations during the daytime. Another aromatic species, naphthalene, showed similar diurnal profile as toluene, but daytime concentrations of naphthalene decreased more significantly than toluene relative to nighttime, which is as the result of higher reactivity for naphthalene (k_{OH}=2.44×10^{-11} cm^3 molecule^{-1} s^{-1}) than toluene (k_{OH}=5.63×10^{-12} cm^3 molecule^{-1} s^{-1}). The diurnal variations of aromatics with different reactivity along with CO are normalized to the midnight values for comparison, as shown in Figure 2(a). We can clearly observe higher daytime removal fractions for more reactive species. To further quantify this behavior, we determine the concentration ratios between measurements at 14:00 and at 6:00-8:00 for measured hydrocarbons during the campaign. The daytime removal fractions as a function of OH rate constants of hydrocarbons are shown in Figure 2(b). Again, the daytime removal fractions increasing with larger OH rate constants are observed, with the largest daytime removal rate up to 70-80% for highly reactive species, e.g. styrene and internal alkenes. Following the work of de Gouw et al. (2009), an exponential curve (y=A×(1-exp(-k_{VOC}[OH]t) is used to fit the data points in Figure 2(b), yielding an OH exposure of 7.2 ±1.7×10^{10} molecule cm^{-3} s. The derived OH exposure corresponds to an average OH concentration of 3.3±0.8×10^6 molecule cm^{-3} between 8:00-14:00. The estimated OH concentration is in good agreement with simulated average OH concentration during the same period using an observation-constrained box model (3.4×10^6 molecule cm^{-3}) (Figure 2a). The encouraging result suggests that the variations of hydrocarbons with different reactivity in the daytime could provide an approach to estimate OH concentrations in the atmosphere.

In addition to primary emissions, OVOCs can also be secondarily produced in the atmosphere from oxidations of other VOCs. Diurnal profiles of selected OVOCs,

https://doi.org/10.5194/acp-2020-152
Preprint. Discussion started: 7 May 2020


Atmospheric Chemistry and Physics Discussions

including formaldehyde, acetone and methanol, are also shown in Figure 1 and Figure 2. Apparently, both formaldehyde and acetone had the highest concentrations in the afternoon, with daytime enhancement ratios of 1.61 and 1.45, respectively. The diurnal variations of formaldehyde and acetone indicate that secondary formation contributed significantly to their concentrations during the campaign. Different from formaldehyde and acetone, no daytime enhancement was observed for methanol. The diurnal profile of methanol follows well with other species with similar low reactivity, e.g. CO and benzene, indicating methanol is mainly contributed by primary emissions. In addition to the three common OVOCs species, the diurnal profile of cresol, one of the first-generation oxidation products of toluene (Schwantes et al., 2016), is also shown in Figure 1. As a highly reactive species (4.1-5.9×10^{-11} cm^3 $molecule^{-1}$ s^{-1} for different isomers), cresol concentrations show large enhancement in the afternoon, indicating strong secondary formation during the daytime. A minor peak of cresol is also observed in the evening, when other primary species also increased, possibly due to traffic emissions during this period. It implies that cresol may also be emitted by primary sources, e.g. vehicle exhausts.

Biogenic emissions are also an important source of VOCs, with isoprene as one of the largest components (Guenther et al., 2012). According to Figure 1, a regular diurnal profile is observed for isoprene, with the highest concentration around noon. The two oxidation products of isoprene, methyl vinyl ketone (MVK) and methacrolein (MACR) were measured as the sum by PTR-ToF-MS. MVK+MACR showed similar diurnal variation as isoprene, with somewhat later peak time than isoprene.

Another interesting VOCs species included in Figure 1 is furan (C_4H_4O). Furan produces the ions with the same nominal mass as isoprene (m/z 69) in PTR-MS, preventing its detection using the traditional quadrupole PTR-MS. A number of PTR-ToF-MS applications have allowed the detection of furan in biomass burning plumes or air strongly influence by biomass burning (Sarkar et al., 2016;Koss et al., 2018;Coggon et al., 2019). Here, an average concentration of 0.05±0.03 ppb for furan was observed during the campaign. Diurnal variation of furan shows a peak concentration in the evening (~20:00), with gradually decreased concentrations for the whole night,

https://doi.org/10.5194/acp-2020-152
Preprint. Discussion started: 7 May 2020


Atmospheric Chemistry and Physics Discussions

253 suggesting a strong evening source for furan and slow removal in the nighttime. The
254 variations of furan concentrations during the daytime are small. Considering that furan
255 is highly reactive (4.2×10^{-11} cm^3 $molecule^{-1}$ s^{-1}), it implies that secondary formation
256 contributed significantly to furan during the daytime.

257 3.2 Analysis of PTR-ToF-MS mass spectra

258 In addition to the typical individual VOCs discussed above, signals of many ions
259 from different VOCs were observed in PTR-ToF-MS mass spectra during this campaign.
260 A peak list with more than 1700 ions was used to perform high-resolution peak fittings
261 from the mass spectra of PTR-ToF-MS, among of which 462 ions had noticeable
262 concentrations in the atmosphere after performing background correction. As discussed
263 in section 2.2, a total of 31 VOCs species were calibrated using either gas cylinders or
264 liquid standards. As shown in Figure S6, the calibration factors of most VOCs species
265 are basically around 4000 cps/ppb, except for the species that are known to be
266 associated with lower sensitivity, due to either proton affinities of those species close
267 to water (e.g. formaldehyde), or easily fragmenting to smaller masses (e.g. ethanol)
268 (Koss et al., 2017). We also tried the method proposed in Sekimoto et al. (2017), but no
269 clear relationship between calibration factors and their capture kinetic rate constants
270 was derived. Therefore, we used the average calibration factor of 4170 cps/ppb to
271 quantify those species without external calibration measured by PTR-ToF-MS.

272 The average mass spectra of PTR-ToF-MS during this campaign expressed in
273 concentration is shown in Figure 3. We divided the VOCs measured by PTR-ToF-MS
274 into groups according to the oxygen atoms in the formula, i.e. "C_xH_y", "$C_xH_yO_1$",
275 "$C_xH_yO_2$", "$C_xH_yO_{\geqslant3}$", "N/S-containing", representing hydrocarbon species (without S
276 or N), OVOCs with one oxygen atom, OVOCs with two oxygen atoms, OVOCs with
277 three or more oxygen atoms, and species containing nitrogen and/or sulfur, respectively.
278 OVOCs related ions dominated the mass spectra of PTR-ToF-MS with an average
279 contribution of 77.2%, which mainly contained one oxygen (54.1%) and two oxygen
280 (22.0%) compounds (Figure 4a). OVOCs with one oxygen atom are mainly contributed
281 by common OVOCs, e.g. formaldehyde, acetaldehyde, methanol, ethanol, acetone,

https://doi.org/10.5194/acp-2020-152
Preprint. Discussion started: 7 May 2020


Atmospheric Chemistry and Physics Discussions

MVK+MACR and methyl ethyl ketone (MEK), which totally accounts for 91% of OVOCs with one oxygen atom (Figure S7). The fraction of $C_xH_yO_{\geqslant 3}$ in the PTR-ToF-MS mass spectra is quite low (1.05%). The low contributions from OVOCs with three or more oxygen atoms are different from the concurrent observations of iodide ToF-CIMS during the campaign, which observed higher fractions of $C_xH_yO_{\geqslant 3}$ than $C_xH_yO_2$ in the mass spectra. These results indicate that OVOCs with more than two oxygen atoms may be underestimated by PTR-ToF-MS, possibly as the result of losses to the inlet of PTR-ToF-MS instrument used in this study (Riva et al., 2019).

Diurnal variations and concentration ratios of daytime (6:00-18:00) relative to nighttime (18:00-6:00) for different categories of ions measured by PTR-ToF-MS are presented in Figure 4(b) and Figure 5, respectively. The "C_xH_y" and "N/S-containing" ions have similar diurnal profiles to hydrocarbons (Figure 1), indicating they are mainly from primary emissions. The different categories of OVOCs have similar diurnal profiles with higher concentrations in the daytime, and the enhancement ratio of concentration increases with the larger oxygen atom number, indicative of higher contributions from the secondary formation for these more oxidized species.

Combining measurements of different VOCs groups by GC-MS/FID and PTR-ToF-MS, we analyze their relative importance in VOCs speciation. The total concentration of OVOCs is 44.3±3.2 ppb, which is significantly higher than alkanes (19.5±1.4 ppb), alkenes+acetylene (4.7±0.7 ppb) and aromatics (4.4±0.5 ppb). The average contribution of OVOCs to the total measured VOCs is determined to be 57.4% during the campaign (Figure 4c-d). This result stresses that OVOCs are important components in VOCs in the urban atmosphere. The fractions of OVOCs in total VOCs shown here is significantly higher than previous results, which usually demonstrates the dominant contribution from hydrocarbons to VOCs in urban air (Yang et al., 2018;Li et al., 2019). The higher OVOCs fraction determined in the study is the result of taking into account the signals from uncalibrated species in mass spectra of PTR-ToF-MS. If only considering the six common OVOCs measured by PTR-MS, i.e. formaldehyde, acetaldehyde, methanol, acetone, MEK and MVK+MACR, the OVOCs fraction in total VOCs would be only 38.9%. It suggests the valuable information provided by PTR-

https://doi.org/10.5194/acp-2020-152
Preprint. Discussion started: 7 May 2020


Atmospheric Chemistry and Physics Discussions

312 ToF-MS in characterizing VOC compositions in urban air.

313 ### 3.3 Source analysis of OVOCs

314 The variations of OVOCs concentrations are influenced by the boundary layer
315 effects, primary emissions, secondary formation and chemical removal processes. Here,
316 a photochemical age-based parameterization method (de Gouw, 2005;de Gouw et al.,
317 2018;Yuan et al., 2012) was used to quantify the contributions of primary anthropogenic
318 emissions, secondary anthropogenic formation, biogenic emissions and background to
319 concentrations of various OVOCs. The photochemical age-based parameterization
320 method for source analysis of OVOCs is based on the following assumptions: (1) the
321 amount of each OVOCs emitted is proportional to an inert tracer (e.g. CO and acetylene
322 C_2H_2); (2) the chemical removal of OVOCs is dominated by reactions with OH radicals;
323 (3) the photochemical age can be calculated using the ratios of two hydrocarbons that
324 react at different rates with OH radicals; (4) biogenic sources of OVOCs are
325 proportional to emissions of isoprene (de Gouw et al., 2005). Based on the above
326 assumptions, the concentration of OVOCs can be expressed by Eq. 1:

327 $$[\mathrm{OVOC}] = ER_{OVOC} \times [C_2H_2] \times \exp\left(-\left(k^*_{OVOC} - k_{C_2H_2}\right)[OH]\Delta t\right)$$

328 $$+ER_{precursor} \times [C_2H_2] \times \frac{k_{precursor}}{k^*_{OVOC} - k_{precursor}}$$

329 $$\times \frac{\exp\left(-k_{precursor}[OH]\Delta t\right) - \exp\left(-k^*_{OVOC}[OH]\Delta t\right)}{\exp\left(-k_{C_2H_2}[OH]\Delta t\right)}$$

330 $$+ER_{biogenic} \times Isoprene_{source} + [background] \quad (1)$$

331 Where ER_{OVOC} and $ER_{precursor}$ are emission ratios versus C_2H_2 for the OVOC
332 and their precursors. $k_{C_2H_2}$ and $k_{precursor}$ are OH rate constants of C_2H_2 and OVOC
333 precursors, respectively. k^*_{OVOC} is the rate constant of OVOC representing the
334 combined loss to reaction with OH radicals and photolysis. $[C_2H_2]$ is the
335 concentration of acetylene, as the tracer for primary anthropogenic sources. CO can
336 also be used as the primary anthropogenic tracer. The fitting results using CO would be
337 similar as acetylene, considering the good correlation between CO and acetylene
338 (R=0.93, slope=6.62 ppb/ppm, Figure S10). $ER_{biogenic}$ is the emission ratio of

https://doi.org/10.5194/acp-2020-152
Preprint. Discussion started: 7 May 2020

Atmospheric Chemistry and Physics Discussions

OVOCs to isoprene from biogenic emissions. $Isoprene_{source}$ is calculated from concentrations of isoprene and its photochemical products MVK and MACR (Apel et al., 2002;Stroud et al., 2001) (see details in SI). $[background]$ is the background concentration of OVOCs. $[OH]\Delta t$ is the OH exposure which is calculated from the ratios between concentrations of m+p-xylene and ethylbenzene (Yuan et al., 2013).

$$[OH]\Delta t = \frac{1}{k_X - k_E} \times \left[ln\frac{[X]}{[E]}|_{t=0} - ln\frac{[X]}{[E]} \right] \quad (2)$$

Where k_X and k_E are rate constants of m+p-xylene and ethylbenzene, respectively. $\frac{[X]}{[E]}|_{t=0}$ is the initial concentration ratio of m+p-xylene /ethylbenzene in fresh emissions (4.0 ppb/ppb, Figure S11) . $\frac{[X]}{[E]}$ is the measured concentration ratio of m+p-xylene /ethylbenzene.

The chemical losses caused by photolysis cannot be ignored for many OVOCs, e.g. formaldehyde (de Gouw et al., 2018). Therefore, the effective rate constant k^*_{OVOC} is used to represent the combined loss of OH oxidation and photolysis, which can be considered as a correction factor (f) for their OH rate constant (Table 1 and Table S2, see details in SI for the calculation using Eq. 3).

$$k^*_{OVOC} = k_{OVOC} + \frac{j_{OVOC}}{[OH]} = k_{OVOC}\left(1 + \frac{j_{OVOC}}{[OH]k_{OVOC}}\right) = f \times k_{OVOC} \quad (3)$$

The fitting results using Eq. 1 for formaldehyde and acetone are shown in Figure 6. The calculated concentrations of the two OVOCs from the four parts in Eq. 1 compared well with measured concentrations, with correlation coefficients of 0.70 and 0.69, respectively. Most of the formaldehyde concentrations are attributed to anthropogenic secondary (31%) and biogenic sources (36%), with minor contributions from primary anthropogenic emissions (9%). The background level of formaldehyde was determined to be 0.16±0.33 ppb, accounting for 24% of its concentration. Acetone concentrations are dominated by anthropogenic primary emission (53%), consistent with previous studies (Yuan et al., 2012;Wang et al., 2014a;Sahu and Saxena, 2015). The fitting results for other typical OVOCs are shown in Table 2 and Table 3. The correlation coefficients between measured and calculated concentrations of OVOCs species are relatively high (0.63-0.76). Overall, the contributions of secondary

https://doi.org/10.5194/acp-2020-152
Preprint. Discussion started: 7 May 2020


Atmospheric Chemistry and Physics Discussions

367 formation from anthropogenic emissions are important for aldehydes (31-44%), while
368 ketones are mainly from primary anthropogenic emissions, with small contributions
369 from secondary formation of anthropogenic sources. Alcohols have significant fractions
370 from primary anthropogenic emission with no observed anthropogenic secondary
371 formation, in good agreement with results in other regions (de Gouw et al., 2005;Yuan
372 et al., 2012). Biogenic sources account for 7-36% of concentrations of different OVOCs,
373 generally with larger fractions for aldehydes (19-36%).

374 The photochemical age-parameterization method has only been used for source
375 analysis of individual OVOCs species. Here, we attempt to use this method to explore
376 the sources of different categories of OVOC ions in PTR-ToF-MS mass spectra, i.e.
377 $C_xH_yO_1$, $C_xH_yO_2$ and $C_xH_yO_{\geq 3}$. An effective OH rate constant of 2×10^{-11} cm^3 $molecule^{-1}$ s^{-1} was applied for different ion groups. The fitting results are also listed in Table 2
379 and Table 3. It is observed that all categories of OVOCs have significantly secondary
380 anthropogenic sources. OVOCs with one oxygen had similar contributions from
381 primary emissions and secondary formation of anthropogenic sources. The determined
382 results show that OVOCs with two oxygen atoms are more secondary than those with
383 one oxygen atom. Primary anthropogenic emission only accounts for minor
384 contribution to OVOCs with three or more oxygen atoms. These results are in
385 accordance with the fact that primary emissions are more reducing. The fractions from
386 biogenic sources to the OVOCs categories are all significant, consistent with the results
387 of individual OVOCs species discussed above. It should be noted that a substantial
388 fraction of OVOCs with three or more oxygen atoms is attributed to the background,
389 which may be due to the tubing delay effects as the result of gas-wall partitioning of
390 these lower volatility multifunctional species (Pagonis et al., 2017).

391 ### 3.4 OH reactivity

392 The oxidation and removal of VOCs depend on the reactivity of VOCs with both
393 ozone and hydroxyl radicals during daytime and the nitrate radical during nighttime
394 (Sarkar et al., 2016). VOCs reactivity can visually and effectively characterize the
395 contributions of various VOCs to atmospheric chemical reactions that are related to the

https://doi.org/10.5194/acp-2020-152
Preprint. Discussion started: 7 May 2020


Atmospheric Chemistry and Physics Discussions

formation of secondary pollutants. A number of previous studies showed significantly missing reactivity between measured and calculated OH reactivities from measured air pollutants (Yang et al., 2016;Whalley et al., 2016). However, this missing fraction can also depend on the individual compounds that are taken into account for the calculated OH reactivity (Pfannerstill et al., 2019). The total OH reactivity is calculated as follows：

$$k_{OH} = k_{CO}[CO] + k_{NO}[NO] + k_{NO_2}[NO_2] + k_{SO_2}[SO_2] + k_{O_3}[O_3] + k_{CH_4}[CH_4] + \sum_i^n k_{VOC_i}[VOC_i]$$

Where k_{CO}, k_{NO}, k_{NO_2}, k_{SO_2}, k_{O_3}, k_{CH_4} and k_{voc_i} are the rate constants between OH radicals and CO, NO, NO_2, SO_2, O_3, CH_4 and VOC species, respectively. $[CO]$, $[NO]$, $[NO_2]$, $[SO_2]$, $[O_3]$, $[CH_4]$ and $[\mathrm{VOC}_i]$ are the measured concentration of CO, NO, NO_2, SO_2, O_3, CH_4 and various VOC species, respectively.

The rate constants for various VOCs are taken from previous literatures (Atkinson and Arey, 2003;Atkinson et al., 2004;Atkinson et al., 2006;Koss et al., 2018). The species taken into account for calculating OH reactivity and their reaction rate constants are listed in Table S3 and Table S4, including all the hydrocarbons measured by GC-MS/FID and 158 species measured by PTR-ToF-MS. The considered VOCs species in the calculation of OH reactivity account for 91.1% of the total VOCs concentration shown in Figure 4 and Table S4. Other VOC species from PTR-ToF-MS were not considered due to the lack of their rate constants with OH radical. Figure 7 shows the comparison of measured OH reactivity by the CRM method and calculated OH reactivity during the campaign. The variations of the measured OH reactivity are generally controlled by anthropogenic species, as indicated by the strong correlation between measured OH reactivity with CO (R=0.63) and also the similar diurnal profile as anthropogenic VOCs species (Figure 7b and Figure 1).

On average, CH_4 and inorganic gases, mainly NO_x and CO, contribute 47.9% of the measured OH reactivity. The hydrocarbons measured by the online GC-MS/FID account for 15.1% of the measured OH reactivity. Another 8.2% of the measured OH reactivity is contributed by a total of nine OVOCs species calibrated for PTR-ToF-MS in this study, including the six common OVOCs quantified by PTR-MS instruments,

https://doi.org/10.5194/acp-2020-152
Preprint. Discussion started: 7 May 2020


Atmospheric Chemistry and Physics Discussions

425 acrolein, pentanone and hexanones (Table S4). In total, the above three groups of
426 compounds explain an average of 71.2% of measured OH reactivity, leaving the
427 remaining 28.8% of the OH reactivity unaccounted during the campaign. This fraction
428 of unaccounted OH reactivity is generally comparable to the results in previous studies
429 that took into account similar VOCs species measured in the urban atmosphere (Yang
430 et al., 2016).

431 As discussed in section 3.2, concentrations of a large number of uncalibrated
432 VOCs are quantified from the signals in PTR-ToF-MS mass spectra. After considering
433 these VOCs to the calculated OH reactivity, the hydrocarbon masses and OVOCs
434 masses from PTR-ToF-MS can account for additional 4.9% and 11.1% of the measured
435 OH reactivity (Figure 7). Note that the contribution of hydrocarbon masses from PTR-
436 ToF-MS also include the contributions from higher alkanes (0.93%) measured by NO+
437 chemistry (Table S4). Nitrogen and sulfur-containing masses only represent a small
438 fraction (0.7%) in OH reactivity. Adding up these contributions, it significantly narrows
439 the gap between the measured and calculated OH reactivity, leaving only 12.1% of OH
440 reactivity as "missing" during the campaign, well below the estimated uncertainty (20%)
441 for the OH reactivity measurements by the CRM method. The results emphasize the
442 important role of PTR-ToF-MS measurements in quantifying and characterizing
443 reactive VOCs species that can lead to ozone and SOA formation. On the basis of Figure
444 7, that the fraction of OVOCs in OH reactivity can be up to 20%, which is comparable
445 to the summed contribution from hydrocarbons measured by both GC-MS/FID and
446 PTR-ToF-MS. These results also highlight the significant contribution of OVOCs in
447 OH reactivity in urban air.

448 In order to gain more knowledge on potential sources of the remaining missing
449 OH reactivity, the diurnal variation of the missing reactivity is plotted in Figure 8a,
450 which illustrates the highest missing reactivity in the morning and evening. This diurnal
451 profile is similar to many hydrocarbons (e.g. ethene and toluene) that are emitted by
452 primary anthropogenic sources. Moderate correlations between the missing reactivity
453 with the reactivities from ethene and NMHCs are also obtained (Figure 8 and Figure
454 S14), while the correlation with OVOCs is substantially weaker, again suggesting that

https://doi.org/10.5194/acp-2020-152
Preprint. Discussion started: 7 May 2020


Atmospheric Chemistry and Physics Discussions

the missing reactivity is more likely due to primary emissions. As the measurement site is in the downtown of Guangzhou with strong influence from vehicle emissions, the unique diurnal variations with higher missing reactivity in morning and evening rush hours indicate that vehicle emissions may play a role. Previous ambient measurement in Nashville, U.S. and at a coastal site in UK also implied the missing reactivity might be due to reactive primary species from anthropogenic sources (e.g. alkenes or aromatics) (Kovacs et al., 2003;Lee et al., 2009). A recent study on gasoline evaporation also suspected branched alkenes that are not routinely detected by GC-MS may contribute significantly to OH reactivity (Wu et al., 2015). As most of the species measured by PTR-ToF-MS have been taken into account for the OH reactivity calculation, reducing the remaining missing reactivities would only be possible with the help from other VOCs measurement techniques, e.g. GC×GC method, which already demonstrated to measure many novel hydrocarbons present in urban air (Xu et al., 2003;Dunmore et al., 2015).

4 Conclusions

In this study, we continuously measured VOCs and OH reactivity using state-of-the-art online instruments at an urban site in Guangzhou in September-November of 2018. Diurnal profile analysis of hydrocarbons show that more reactive hydrocarbons are associated with stronger chemical removal by OH radicals during the daytime. This relationship is used to estimate the daytime average OH radical concentration, obtaining good agreement with the simulation result of a box model. Diurnal profiles of OVOCs (e.g. formaldehyde and acetone) show large enhancement in the afternoon, indicating contributions from the secondary formation during the daytime. A photochemical age-based parameterization method is used to analyze sources of OVOC in the atmosphere. We find that secondary formation is generally important for aldehydes, while primary emissions from anthropogenic sources dominated the concentrations of ketones.

During the campaign, around 1700 ions were detected in PTR-ToF-MS mass spectra, among of which 462 ions are with noticeable concentrations in the atmosphere. We further quantify VOCs concentrations from signals of 431 ions in mass spectra of

https://doi.org/10.5194/acp-2020-152
Preprint. Discussion started: 7 May 2020


Atmospheric Chemistry and Physics Discussions

PTR-ToF-MS that are not explicitly calibrated, based on the calibrated sensitivities of more than 30 VOCs species. The analyses indicate that OVOC-related ions dominated PTR-ToF-MS mass spectra with an average contribution of 77.2%, mainly compounds with one (54.1%) and two oxygen atoms (22.0%). Source analyses of these different categories of OVOCs from PTR-ToF-MS also show that these OVOCs are contributed by both primary and secondary sources. Combining measurements from PTR-ToF-MS and GC-MS/FID, OVOCs contribute 57.4% to the total concentration of VOCs, indicating the important roles of OVOCs.

Finally, we find OVOCs measured by PTR-ToF-MS contribute greatly to the OH reactivity (19.3%), with 8.2% from common OVOCs that are explicitly calibrated and 11.1% from other newly-quantified OVOCs signals in the mass spectra. In comparison, hydrocarbons account for 20.0% of OH reactivity during the campaign, with 15.1% from hydrocarbons measured by GC-MS/FID and 4.9% by PTR-ToF-MS, respectively. Adding up the contributions from inorganic gases (47.9%), the missing reactivity is estimated to be 12.1%. Evidence from diurnal variations and correlation analysis indicates that the missing reactivity is most likely due to hydrocarbons from primary emitted by anthropogenic sources.

In summary, our VOCs measurements at an urban site in Guangzhou demonstrate the important contributions of OVOCs to both total VOCs concentrations and OH reactivity in the atmosphere. As urban emissions are transported downwind, contributions from OVOCs in the urban emissions should continuously increase (de Gouw et al., 2005). It highlights that OVOCs play important roles in VOCs emissions and chemistry in urban air. In this study, concentrations of most OVOCs are quantified by a PTR-ToF-MS instruments, indicating the usefulness of PTR-ToF-MS in characterizing VOCs emission and chemistry in the atmosphere. Nevertheless, our analysis on OH reactivity implies potential contributions from highly reactive hydrocarbons that are not captured by neither GC-MS/FID nor PTR-ToF-MS, calling for other measurement techniques for VOCs to fill this gap.

Acknowledgements

https://doi.org/10.5194/acp-2020-152
Preprint. Discussion started: 7 May 2020

Atmospheric Chemistry and Physics Discussions

513 This work was supported by the National Key R&D Plan of China (grant No.
514 2018YFC0213904, 2016YFC0202206), the National Natural Science Foundation of
515 China (grant No. 41877302), Guangdong Natural Science Funds for Distinguished
516 Young Scholar (grant No. 2018B030306037), Guangdong Provincial Key R&D Plan
517 (grant No. 2019B110206001), Guangdong Soft Science Research Program (grant No.
518 2019B101001005) and Guangdong Innovative and Entrepreneurial Research Team
519 Program (grant No. 2016ZT06N263). Weiwei Hu was supported by National Natural
520 Science Foundation of China (grant No. 41875156). The authors gratefully
521 acknowledge the science team for their technical support and discussions during the
522 campaigns in PRD.

523

https://doi.org/10.5194/acp-2020-152
Preprint. Discussion started: 7 May 2020

Atmospheric Chemistry and Physics Discussions

References

Apel, E. C., Riemer, D. D., Hills, A., Baugh, W., Orlando, J., Faloona, I., Tan, D., Brune, W., Lamb, B., Westberg, H., Carroll, M. A., Thornberry, T., and Geron, C. D.: Measurement and interpretation of isoprene fluxes and isoprene, methacrolein, and methyl vinyl ketone mixing ratios at the PROPHET site during the 1998 Intensive, Journal of Geophysical Research: Atmospheres, 107, ACH 7-1-ACH 7-15, 10.1029/2000jd000225, 2002.

Atkinson, R., and Arey, J.: Atmospheric Degradation of Volatile Organic Compounds, Chemical Reviews, 103, 4605-4638, 10.1021/cr0206420, 2003.

Atkinson, R., Baulch, D. L., Cox, R. A., Crowley, J. N., Hampson, R. F., Hynes, R. G., Jenkin, M. E., Rossi, M. J., and Troe, J.: Evaluated kinetic and photochemical data for atmospheric chemistry: Volume I - gas phase reactions of Ox, HOx, NOx and SOx species, Atmos. Chem. Phys., 4, 1461-1738, 10.5194/acp-4-1461-2004, 2004.

Atkinson, R., Baulch, D. L., Cox, R. A., Crowley, J. N., Hampson, R. F., Hynes, R. G., Jenkin, M. E., Rossi, M. J., Troe, J., and Subcommittee, I.: Evaluated kinetic and photochemical data for atmospheric chemistry: Volume II – gas phase reactions of organic species, Atmos. Chem. Phys., 6, 3625-4055, 10.5194/acp-6-3625-2006, 2006.

Cappellin, L., Karl, T., Probst, M., Ismailova, O., Winkler, P., Soukoulis, C., Aprea, E., Märk, T., Gasperi, F., and Biasioli, F.: On Quantitative Determination of Volatile Organic Compound Concentrations Using Proton Transfer Reaction Time-of-Flight Mass Spectrometry, Environmental science & technology, 46, 2283-2290, 10.1021/es203985t, 2012.

Coggon, M. M., Lim, C. Y., Koss, A. R., Sekimoto, K., Yuan, B., Gilman, J. B., Hagan, D. H., Selimovic, V., Zarzana, K. J., Brown, S. S., Roberts, J. M., Müller, M., Yokelson, R., Wisthaler, A., Krechmer, J. E., Jimenez, J. L., Cappa, C., Kroll, J. H., de Gouw, J., and Warneke, C.: OH chemistry of non-methane organic gases (NMOGs) emitted from laboratory and ambient biomass burning smoke: evaluating the influence of furans and oxygenated aromatics on ozone and secondary NMOG formation, Atmos. Chem. Phys., 19, 14875-14899, 10.5194/acp-19-14875-2019, 2019.

de Gouw, J., Middlebrook, A., warneke, C., Goldan, P., Kuster, W., Roberts, J., Fehsenfeld, F., Worsnop, D., Pszenny, A., Keene, W., Marchewka, M., Bertman, S., and Bates, T.: Budget of organic carbon in a polluted atmosphere: Results from the New England Air Quality Study in 2002, Journal of Geophysical Research-Atmospheres, 110, D16305, 10.1029/2004JD005623, 2005.

de Gouw, J., and Warneke, C.: Measurements of volatile organic compounds in the earth's atmosphere using proton-transfer-reaction mass spectrometry, Mass Spectrometry Reviews, 26, 223-257, 10.1002/mas.20119, 2007.

de Gouw, J., Welsh-Bon, D., warneke, C., Kuster, W., Laskin, A., Baker, A., Beyersdorf, A., Blake, D., Canagaratna, M., Celada Murillo, A. T., Huey, L., Junkermann, W., Onasch, T., Salcido, A., Sjostedt, S., Sullivan, A., Tanner, D., Vargas, O., Weber, R., and Zaveri, R.: Emission and chemistry of organic carbon in the gas and aerosol phase at a sub-urban site near Mexico City in March 2006 during the MILAGRO study, ATMOSPHERIC CHEMISTRY AND PHYSICS, 9, 3425-3442, 10.5194/acp-9-3425-

https://doi.org/10.5194/acp-2020-152
Preprint. Discussion started: 7 May 2020


Atmospheric Chemistry and Physics Discussions

2009, 2009.
de Gouw, J. A.: Budget of organic carbon in a polluted atmosphere: Results from the New England Air Quality Study in 2002, Journal of Geophysical Research, 110, 10.1029/2004jd005623, 2005.
de Gouw, J. A., Gilman, J. B., Kim, S. W., Lerner, B. M., Isaacman-VanWertz, G., McDonald, B. C., Warneke, C., Kuster, W. C., Lefer, B. L., Griffith, S. M., Dusanter, S., Stevens, P. S., and Stutz, J.: Chemistry of Volatile Organic Compounds in the Los Angeles basin: Nighttime Removal of Alkenes and Determination of Emission Ratios, Journal of Geophysical Research: Atmospheres, 122, 11,843-811,861, 10.1002/2017jd027459, 2017.
de Gouw, J. A., Gilman, J. B., Kim, S.-W., Alvarez, S. L., Dusanter, S., Graus, M., Griffith, S. M., Isaacman-VanWertz, G., Kuster, W. C., Lefer, B. L., Lerner, B. M., McDonald, B. C., Rappenglück, B., Roberts, J. M., Stevens, P. S., Stutz, J., Thalman, R., Veres, P. R., Volkamer, R., Warneke, C., Washenfelder, R. A., and Young, C. J.: Chemistry of Volatile Organic Compounds in the Los Angeles Basin: Formation of Oxygenated Compounds and Determination of Emission Ratios, Journal of Geophysical Research: Atmospheres, 123, 2298-2319, 10.1002/2017jd027976, 2018.
Dolgorouky, C., Gros, V., Sarda-Esteve, R., Sinha, V., Williams, J., Marchand, N., Sauvage, S., Poulain, L., Sciare, J., and Bonsang, B.: Total OH reactivity measurements in Paris during the 2010 MEGAPOLI winter campaign, Atmos. Chem. Phys., 12, 9593-9612, 10.5194/acp-12-9593-2012, 2012.
Dunmore, R., Hopkins, J., Lidster, R., Lee, J., Evans, M., Rickard, A., Lewis, A., and Hamilton, J.: Diesel-related hydrocarbons can dominate gas phase reactive carbon in megacities, Atmospheric Chemistry and Physics, 15, 10.5194/acp-15-9983-2015, 2015.
Ferracci, Valerio, Heimann, Ines, Abraham, N., Luke, Pyle, John, and A.: Global modelling of the total OH reactivity: investigations on the "missing" OH sink and its atmospheric implications, 2018.
Fry, M., Schwarzkopf, M., Adelman, Z., and West, J.: Air quality and radiative forcing impacts of anthropogenic volatile organic compound emissions from ten world regions, ATMOSPHERIC CHEMISTRY AND PHYSICS, 14, 10.5194/acp-14-523-2014, 2013.
Gentner, D., Worton, D., Isaacman, G., Davis, L., Dallmann, T., Wood, E., Herndon, S., Goldstein, A., and Harley, R.: Chemical Composition of Gas-Phase Organic Carbon Emissions from Motor Vehicles and Implications for Ozone Production, Environmental science & technology, 47, 10.1021/es401470e, 2013.
Gilman, J., Lerner, B., Kuster, W., and de Gouw, J.: Source Signature of Volatile Organic Compounds from Oil and Natural Gas Operations in Northeastern Colorado, Environmental science & technology, 47, 10.1021/es304119a, 2013.
Gilman, J. B., Lerner, B. M., Kuster, W. C., Goldan, P. D., Warneke, C., Veres, P. R., Roberts, J. M., de Gouw, J. A., Burling, I. R., and Yokelson, R. J.: Biomass burning emissions and potential air quality impacts of volatile organic compounds and other trace gases from fuels common in the US, Atmospheric Chemistry and Physics, 15, 13915-13938, 10.5194/acp-15-13915-2015, 2015.
Guenther, A., Jiang, J., Heald, C., Sakulyanontvittaya, Duhl, T., Emmons, L., and Wang, J.: The Model of Emissions of Gases and Aerosols from Nature version 2.1

https://doi.org/10.5194/acp-2020-152
Preprint. Discussion started: 7 May 2020


Atmospheric Chemistry and Physics Discussions

611 (MEGAN2.1): An extended and updated framework for modeling biogenic emissions,
612 Geoscientific Model Development Discussions, 5, 1-58, 10.5194/gmdd-5-1-2012, 2012.
613 Hansen, R. F., Griffith, S. M., Dusanter, S., Rickly, P. S., Stevens, P. S., Bertman, S. B.,
614 Carroll, M. A., Erickson, M. H., Flynn, J. H., Grossberg, N., Jobson, B. T., Lefer, B. L.,
615 and Wallace, H. W.: Measurements of total hydroxyl radical reactivity during
616 CABINEX 2009 – Part 1: field measurements, Atmos. Chem. Phys., 14, 2923-
617 2937, 10.5194/acp-14-2923-2014, 2014.
618 Holzinger, R., Acton, W., Bloss, W., Breitenlechner, M., Crilley, L., Dusanter, S., Gonin,
619 M., Gros, V., Keutsch, F., Kiendler-Scharr, A., Kramer, L., Krechmer, J., Languille, B.,
620 Locoge, N., Lopez-Hilfiker, F., Materic, D., Moreno, S., Nemitz, E., Quéléver, L., and
621 Zaytsev, A.: Validity and limitations of simple reaction kinetics to calculate
622 concentrations of organic compounds from ion counts in PTR-MS, Atmospheric
623 Measurement Techniques Discussions, 1-29, 10.5194/amt-2018-446, 2019.
624 Kari, E., Miettinen, P., Yli-Pirilä, P., Virtanen, A., and Faiola, C.: PTR-ToF-MS product
625 ion distributions and humidity-dependence of biogenic volatile organic compounds,
626 International Journal of Mass Spectrometry, 430, 10.1016/j.ijms.2018.05.003, 2018.
627 Karl, T., Guenther, A., Turnipseed, A., Tyndall, G., Artaxo, P., and Martin, S.: Rapid
628 formation of isoprene photo-oxidation products observed in Amazonia, Atmos. Chem.
629 Phys., 9, 7753-7767, 10.5194/acp-9-7753-2009, 2009.
630 Kim, K.-H., Hong, Y.-J., Pal, R., Jeon, E.-C., Koo, Y.-S., and Sunwoo, Y.: Investigation
631 of carbonyl compounds in air from various industrial emission sources, Chemosphere,
632 70, 807-820, https://doi.org/10.1016/j.chemosphere.2007.07.025, 2008.
633 Kim, S., Sanchez, D., Wang, M., Seco, R., Jeong, D., Hughes, S., Barletta, B., Blake,
634 D., Jung, J., Kim, D., Lee, G., Lee, M., Ahn, J., Lee, S.-D., Cho, G., Sung, M.-Y., Lee,
635 Y.-H., Kim, D., and Hong, J.-H.: OH Reactivity in Urban and Suburban regions in Seoul,
636 South Korea- An East Asian megacity in a rapid transition, Faraday Discuss., 189,
637 10.1039/C5FD00230C, 2016.
638 Koss, A., Yuan, B., Warneke, C., Gilman, J. B., Lerner, B. M., Veres, P. R., Peischl, J.,
639 Eilerman, S., Wild, R., Brown, S. S., Thompson, C. R., Ryerson, T., Hanisco, T., Wolfe,
640 G. M., Clair, J. M. S., Thayer, M., Keutsch, F. N., Murphy, S., and de Gouw, J.:
641 Observations of VOC emissions and photochemical products over US oil- and gas-
642 producing regions using high-resolution H3O+ CIMS (PTR-ToF-MS), Atmospheric
643 Measurement Techniques, 10, 2941-2968, 10.5194/amt-10-2941-2017, 2017.
644 Koss, A. R., Sekimoto, K., Gilman, J. B., Selimovic, V., Coggon, M. M., Zarzana, K.
645 J., Yuan, B., Lerner, B. M., Brown, S. S., Jimenez, J. L., Krechmer, J., Roberts, J. M.,
646 Warneke, C., Yokelson, R. J., and de Gouw, J.: Non-methane organic gas emissions
647 from biomass burning: identification, quantification, and emission factors from PTR-
648 ToF during the FIREX 2016 laboratory experiment, Atmospheric Chemistry and
649 Physics, 18, 3299-3319, 10.5194/acp-18-3299-2018, 2018.
650 Kovacs, T. A., Brune, W., Harder, H., Martinez, M., Simpas, J., Frost, G., Williams, E.,
651 Jobson, T., Stroud, C., Young, V., Fried, A., and Wert, B.: Direct measurements of urban
652 OH reactivity during Nashville SOS in summer 1999, Journal of environmental
653 monitoring : JEM, 5, 68-74, 10.1039/B204339D, 2003.
654 Lee, J. D., Young, J. C., Read, K. A., Hamilton, J. F., Hopkins, J. R., Lewis, A. C.,

https://doi.org/10.5194/acp-2020-152
Preprint. Discussion started: 7 May 2020

655 Bandy, B. J., Davey, J., Edwards, P., Ingham, T., Self, D. E., Smith, S. C., Pilling, M. J.,
656 and Heard, D. E.: Measurement and calculation of OH reactivity at a United Kingdom
657 coastal site, Journal of Atmospheric Chemistry, 64, 53-76, 10.1007/s10874-010-9171-
658 0, 2009.
659 Li, K., Li, J., Tong, S., Wang, W., Huang, R.-J., and Ge, M.: Characteristics of
660 wintertime VOCs in suburban and urban Beijing: concentrations, emission ratios, and
661 festival effects, Atmospheric Chemistry and Physics, 19, 8021-8036, 10.5194/acp-19-
662 8021-2019, 2019.
663 Lou, S., Holland, F., Rohrer, F., Lu, K., Bohn, B., Brauers, T., Chang, C. C., Fuchs, H.,
664 Häseler, R., Kita, K., Kondo, Y., Li, X., Shao, M., Zeng, L., Wahner, A., Zhang, Y.,
665 Wang, W., and Hofzumahaus, A.: Atmospheric OH reactivities in the Pearl River Delta
666 – China in summer 2006: measurement and model results, Atmos. Chem. Phys., 10,
667 11243-11260, 10.5194/acp-10-11243-2010, 2010.
668 Louie, P. K. K., Ho, J. W. K., Tsang, R. C. W., Blake, D. R., Lau, A. K. H., Yu, J. Z.,
669 Yuan, Z., Wang, X., Shao, M., and Zhong, L.: VOCs and OVOCs distribution and
670 control policy implications in Pearl River Delta region, China, Atmospheric
671 Environment, 76, 125-135, 2013.
672 Mao, J., Ren, X., Chen, S., Brune, W. H., Chen, Z., Martinez, M., Harder, H., Lefer, B.,
673 Rappenglück, B., Flynn, J., and Leuchner, M.: Atmospheric oxidation capacity in the
674 summer of Houston 2006: Comparison with summer measurements in other
675 metropolitan studies, Atmospheric Environment, 44, 4107-4115,
676 https://doi.org/10.1016/j.atmosenv.2009.01.013, 2010.
677 Mellouki, A., Wallington, T. J., and Chen, J.: Atmospheric Chemistry of Oxygenated
678 Volatile Organic Compounds: Impacts on Air Quality and Climate, Chemical Reviews,
679 115, 3984-4014, 10.1021/cr500549n, 2015.
680 Michoud, V., Hansen, R., Locoge, N., Stevens, P., and Dusanter, S.: Detailed
681 characterizations of the new Mines Douai comparative reactivity method instrument via
682 laboratory experiments and modeling, Atmospheric Measurement Techniques, 8, 3537–
683 3553, 10.5194/amt-8-3537-2015, 2015.
684 Millet, D., Baasandorj, M., Farmer, D., Thornton, J., Baumann, K., Brophy, P.,
685 Chaliyakunnel, S., de Gouw, J., Graus, M., Hu, L., Koss, A., Lee, B., Lopez-Hilfiker,
686 F., Neuman, J., Paulot, F., Peischl, J., Pollack, I., Ryerson, T., warneke, C., and Xu, J.:
687 A large and ubiquitous source of atmospheric formic acid, Atmospheric Chemistry and
688 Physics Discussions, 15, 4537-4599, 10.5194/acpd-15-4537-2015, 2015.
689 Pagonis, D., Krechmer, J. E., de Gouw, J., Jimenez, J. L., and Ziemann, P. J.: Effects of
690 gas–wall partitioning in Teflon tubing and instrumentation on time-resolved
691 measurements of gas-phase organic compounds, Atmospheric Measurement
692 Techniques, 10, 4687-4696, 10.5194/amt-10-4687-2017, 2017.
693 Park, J. H., Goldstein, A. H., Timkovsky, J., Fares, S., Weber, R., Karlik, J., and
694 Holzinger, R.: Active atmosphere-ecosystem exchange of the vast majority of detected
695 volatile organic compounds, Science, 341, 643-647, 10.1126/science.1235053, 2013.
696 Pfannerstill, E. Y., Wang, N., Edtbauer, A., Bourtsoukidis, E., Crowley, J. N., Dienhart,
697 D., Eger, P. G., Ernle, L., Fischer, H., Hottmann, B., Paris, J. D., Stönner, C., Tadic, I.,
698 Walter, D., Lelieveld, J., and Williams, J.: Shipborne measurements of total OH

https://doi.org/10.5194/acp-2020-152
Preprint. Discussion started: 7 May 2020


Atmospheric Chemistry and Physics Discussions

reactivity around the Arabian Peninsula and its role in ozone chemistry, Atmos. Chem. Phys., 19, 11501-11523, 10.5194/acp-19-11501-2019, 2019.

Praplan, A. P., Pfannerstill, E. Y., Williams, J., and Hellén, H.: OH reactivity of the urban air in Helsinki, Finland, during winter, Atmospheric Environment, 169, 150-161, https://doi.org/10.1016/j.atmosenv.2017.09.013, 2017.

Ran, L., Zhao, C. S., Xu, W. Y., Lu, X. Q., Han, M., Lin, W. L., Yan, P., Xu, X. B., Deng, Z. Z., Ma, N., Liu, P. F., Yu, J., Liang, W. D., and Chen, L. L.: VOC reactivity and its effect on ozone production during the HaChi summer campaign, Atmos. Chem. Phys., 11, 4657-4667, 10.5194/acp-11-4657-2011, 2011.

Riva, M., Rantala, P., Krechmer, J., Perakyla, O., Zhang, Y., Heikkinen, L., Garmash, O., Yan, C., Kulmala, M., Worsnop, D., and Ehn, M.: Evaluating the performance of five different chemical ionization techniques for detecting gaseous oxygenated organic species, Atmospheric Measurement Techniques, 12, 2403-2421, 10.5194/amt-12-2403-2019, 2019.

Sahu, L. K., and Saxena, P.: High time and mass resolved PTR-TOF-MS measurements of VOCs at an urban site of India during winter: Role of anthropogenic, biomass burning, biogenic and photochemical sources, Atmospheric Research, 164-165, 84-94, https://doi.org/10.1016/j.atmosres.2015.04.021, 2015.

Sarkar, C., Sinha, V., Kumar, V., Rupakheti, M., Panday, A., Mahata, K. S., Rupakheti, D., Kathayat, B., and Lawrence, M. G.: Overview of VOC emissions and chemistry from PTR-TOF-MS measurements during the SusKat-ABC campaign: high acetaldehyde, isoprene and isocyanic acid in wintertime air of the Kathmandu Valley, Atmos. Chem. Phys., 16, 3979-4003, 10.5194/acp-16-3979-2016, 2016.

Schwantes, R., Schilling, K., McVay, R., Lignell, H., Coggon, M., Zhang, X., Wennberg, P., and Seinfeld, J.: Formation of Highly Oxygenated Low-Volatility Products from Cresol Oxidation, Atmospheric Chemistry and Physics Discussions, 1-34, 10.5194/acp-2016-887, 2016.

Sekimoto, K., Li, S.-M., Yuan, B., Koss, A., Coggon, M., Warneke, C., and de Gouw, J.: Calculation of the sensitivity of proton-transfer-reaction mass spectrometry (PTR-MS) for organic trace gases using molecular properties, International Journal of Mass Spectrometry, 421, 71-94, https://doi.org/10.1016/j.ijms.2017.04.006, 2017.

Simpson, I. J., Marrero, J. E., Batterman, S., Meinardi, S., Barletta, B., and Blake, D. R.: Air quality in the Industrial Heartland of Alberta, Canada and potential impacts on human health, Atmospheric Environment, 81, 702-709, https://doi.org/10.1016/j.atmosenv.2013.09.017, 2013.

Sinha, V., Williams, J., Crowley, J. N., and Lelieveld, J.: The Comparative Reactivity Method – a new tool to measure total OH Reactivity in ambient air, Atmos. Chem. Phys., 8, 2213-2227, 10.5194/acp-8-2213-2008, 2008.

Stockwell, C. E., Veres, P. R., Williams, J., and Yokelson, R. J.: Characterization of biomass burning emissions from cooking fires, peat, crop residue, and other fuels with high-resolution proton-transfer-reaction time-of-flight mass spectrometry, Atmos. Chem. Phys., 15, 845-865, 10.5194/acp-15-845-2015, 2015.

Stroud, C. A., Roberts, J. M., Goldan, P. D., Kuster, W. C., Murphy, P. C., Williams, E. J., Hereid, D., Parrish, D., Sueper, D., Trainer, M., Fehsenfeld, F. C., Apel, E. C., Riemer,

https://doi.org/10.5194/acp-2020-152
Preprint. Discussion started: 7 May 2020

743 D., Wert, B., Henry, B., Fried, A., Martinez-Harder, M., Harder, H., Brune, W. H., Li,
744 G., Xie, H., and Young, V. L.: Isoprene and its oxidation products, methacrolein and
745 methylvinyl ketone, at an urban forested site during the 1999 Southern Oxidants Study,
746 Journal of Geophysical Research: Atmospheres, 106, 8035-8046,
747 10.1029/2000jd900628, 2001.
748 Wang, M., Chen, W., Shao, M., Lu, S., Zeng, L., and Hu, M.: Investigation of carbonyl
749 compound sources at a rural site in the Yangtze River Delta region of China, Journal of
750 Environmental Sciences, 28, 10.1016/j.jes.2014.12.001, 2014a.
751 Wang, M., Zeng, L., Lu, S., Shao, M., Liu, X., Yu, X., Chen, W., Yuan, B., Zhang, Q.,
752 Hu, M., and Zhang, Z.: Development and validation of a cryogen-free automatic gas
753 chromatograph system (GC-MS/FID) for online measurements of volatile organic
754 compounds, Anal. Methods, 6, 10.1039/C4AY01855A, 2014b.
755 Whalley, L. K., Stone, D., Bandy, B., Dunmore, R., Hamilton, J. F., Hopkins, J., Lee, J.
756 D., Lewis, A. C., and Heard, D. E.: Atmospheric OH reactivity in central London:
757 observations, model predictions and estimates of in situ ozone production, Atmos.
758 Chem. Phys., 16, 2109-2122, 10.5194/acp-16-2109-2016, 2016.
759 Wolfe, G. M., Thornton, J. A., Bouvier-Brown, N. C., Goldstein, A. H., Park, J. H.,
760 McKay, M., Matross, D. M., Mao, J., Brune, W. H., LaFranchi, B. W., Browne, E. C.,
761 Min, K. E., Wooldridge, P. J., Cohen, R. C., Crounse, J. D., Faloona, I. C., Gilman, J.
762 B., Kuster, W. C., de Gouw, J. A., Huisman, A., and Keutsch, F. N.: The Chemistry of
763 Atmosphere-Forest Exchange (CAFE) Model – Part 2: Application to BEARPEX-2007
764 observations, Atmos. Chem. Phys., 11, 1269-1294, 10.5194/acp-11-1269-2011, 2011.
765 Wu, Y., Yang, Y.-D., Shao, M., and Lu, S.-H.: Missing in total OH reactivity of VOCs
766 from gasoline evaporation, Chinese Chemical Letters, 26, 10.1016/j.cclet.2015.05.047,
767 2015.
768 Xu, X., Williams, J., Plass-Dülmer, C., Berresheim, H., Salisbury, G., Lange, L., and
769 Lelieveld, J.: GC×GC measurements of C7-C11 aromatic and n-alkane hydrocarbons
770 on Crete, in air from Eastern Europe during the MINOS campaign, Atmospheric
771 Chemistry and Physics Discussions, 3, 10.5194/acpd-3-1477-2003, 2003.
772 Yang, Y., Shao, M., Wang, X., Nölscher, A. C., Kessel, S., Guenther, A., and Williams,
773 J.: Towards a quantitative understanding of total OH reactivity: A review, Atmospheric
774 Environment, 134, 147-161, https://doi.org/10.1016/j.atmosenv.2016.03.010, 2016.
775 Yang, Y., Liu, X., Zheng, J., Tan, Q., Feng, M., qu, y., An, J., and Cheng, N.:
776 Characteristics of one-year observation of VOCs, NOx, and O3 at an urban site in
777 Wuhan, China, Journal of Environmental Sciences, 79, 10.1016/j.jes.2018.12.002, 2018.
778 Yuan, B., Shao, M., Gouw, J. D., Parrish, D. D., Lu, S., Wang, M., Zeng, L., Zhang, Q.,
779 Song, Y., and Zhang, J.: Volatile organic compounds (VOCs) in urban air: How
780 chemistry affects the interpretation of positive matrix factorization (PMF) analysis,
781 Journal of Geophysical Research Atmospheres, 117, 24302, 2012.
782 Yuan, B., Hu, W. W., Shao, M., and Wang, M.: VOC emissions, evolutions and
783 contributions to SOA formation at a receptor site in Eastern China, Atmospheric
784 Chemistry & Physics, 13, 8815-8832, 2013.
785 Yuan, B., Koss, A. R., Warneke, C., Coggon, M., Sekimoto, K., and de Gouw, J. A.:
786 Proton-Transfer-Reaction Mass Spectrometry: Applications in Atmospheric Sciences,

https://doi.org/10.5194/acp-2020-152
Preprint. Discussion started: 7 May 2020

Atmospheric Chemistry and Physics Discussions

787 Chemical Reviews, 117, 13187-13229, 10.1021/acs.chemrev.7b00325, 2017.
788

https://doi.org/10.5194/acp-2020-152
Preprint. Discussion started: 7 May 2020

Atmospheric Chemistry and Physics Discussions

789 **Table 1.** Rate constants of OVOCs representing the combined loss to OH and photolysis.

Species	k_{ovoc}	$j_{ovoc}/[OH]$	k^*_{ovoc}	$f^{\#}$
	$cm^3molecule^{-1}s^{-1}$			
Formaldehyde	9.4×10^{-12}	$7.8\times10^{-12}\pm1.2\times10^{-13}$	17.2×10^{-12}	1.83
Acetaldehyde	15×10^{-12}	$4.2\times10^{-13}\pm6.0\times10^{-15}$	15.42×10^{-12}	1.03
Acrolein	19.6×10^{-12}	$4.2\times10^{-13}\pm6.0\times10^{-15}$	20.02×10^{-12}	1.02
Acetone	0.17×10^{-12}	$5.1\times10^{-14}\pm7.2\times10^{-16}$	0.22×10^{-12}	1.29
MEK	1.22×10^{-12}	$3.7\times10^{-13}\pm5.2\times10^{-15}$	1.59×10^{-12}	1.30
Pentanone	7.9×10^{-12}	$3.7\times10^{-13}\pm5.2\times10^{-15}$	8.27×10^{-12}	1.05

790 #: f represents the ratio of the rate constant representing the combined losses of reaction
791 with OH radical and photolysis (k^*_{ovoc}) and the OH rate constant (k_{ovoc}).
792

https://doi.org/10.5194/acp-2020-152
Preprint. Discussion started: 7 May 2020

Atmospheric Chemistry and Physics Discussions

793 **Table 2.** Parameters describing OVOC concentrations.

Species	ER_{OVOC}	$ER_{precursor}$	$k_{precursor}$	$ER_{biogenic}$	Background	ER_{OVOC}[c]
	ppb [ppb C_2H_2]$^{-1}$		10^{-12}cm^3 molecule^{-1} s^{-1}	ppb [ppb isoprene]$^{-1}$	ppbv	ppb [ppm CO]$^{-1}$
Formaldehyde	0.22±0.12	4.49±6.03	4.59±7.22	1.61±0.08	0.66±0.13	1.46
Acetaldehyde	0.66±0.07	3.69±2.31	5.87±4.50	0.62±0.05	0[b]	4.37
Acrolein	0.06±0.01	1.49±8.27	0.87±5.00	0.08±0	0[b]	0.40
Methanol	5.12±0.11	0[b]	0[b]	3.34±0.26	0[b]	33.9
Ethanol	3.08±0.08	0[b]	0[b]	1.11±0.16	0[b]	20.4
Acetone	1.04±0.13	6.96±63.87	1.42±13.8	1.33±0.1	0.28±0.16	6.88
MEK	0.45±0.15	0.47±0.13	56.9±31.3	0.15±0.06	0[b]	2.98
Pentanone	0.03±0	0.41±1.46	1.33±4.94	0.02±0	0[b]	0.20
$C_xH_yO_1$	11.61±1.13	36.66±18.19	8.78±5.88	10.7± 0.74	0[b]	76.9
$C_xH_yO_2$	3.70±0.68	15.72±8.72	9.39±7.32	4.30± 0.38	0[b]	24.5
$C_xH_yO_{\geq 3}$	0.04±0.07	1.45±6.53	3.21±16.2	0.38±0.04	0.25±0.07	0.26

794 [a] The parameters ER_{OVOC}, $ER_{precursor}$, $k_{precursor}$, $ER_{biogenic}$ and background are fitted
795 to the measured concentration data according to equation (1).
796 [b] As the fitting value of the parameter is negative, that parameter is set to zero
797 and the fit is repeated.
798 [c] Emission ratios relative to CO are calculated from emission ratios relative to
799 acetylene multipling the emission ratio of acetylene to CO (6.62 ppb/ppm) (Figure
800 S10).
801

https://doi.org/10.5194/acp-2020-152
Preprint. Discussion started: 7 May 2020

Atmospheric Chemistry and Physics Discussions

802 **Table 3.** Contribution fractions of OVOCs from different sources and correlation
803 coefficient between calculated and measured OVOC concentrations.

Species	Primary Anthropogenic, %	Secondary Anthropogenic, %	Biogenic, %	Background, %	R
Formaldehyde	9	31	36	24	0.70
Acetaldehyde	37	44	19	0	0.76
Acrolein	35	34	31	0	0.74
Methanol	82	0	18	0	0.68
Ethanol	87	0	13	0	0.68
Acetone	53	17	22	8	0.69
MEK	50	43	7	0	0.63
Pentanone	43	35	17	5	0.75
$C_xH_yO_1$	40	38	22	0	0.70
$C_xH_yO_2$	33	43	24	0	0.62
$C_xH_yO_{\geqslant 3}$	6	26	35	33	0.45

804

https://doi.org/10.5194/acp-2020-152
Preprint. Discussion started: 7 May 2020

Atmospheric Chemistry and Physics Discussions

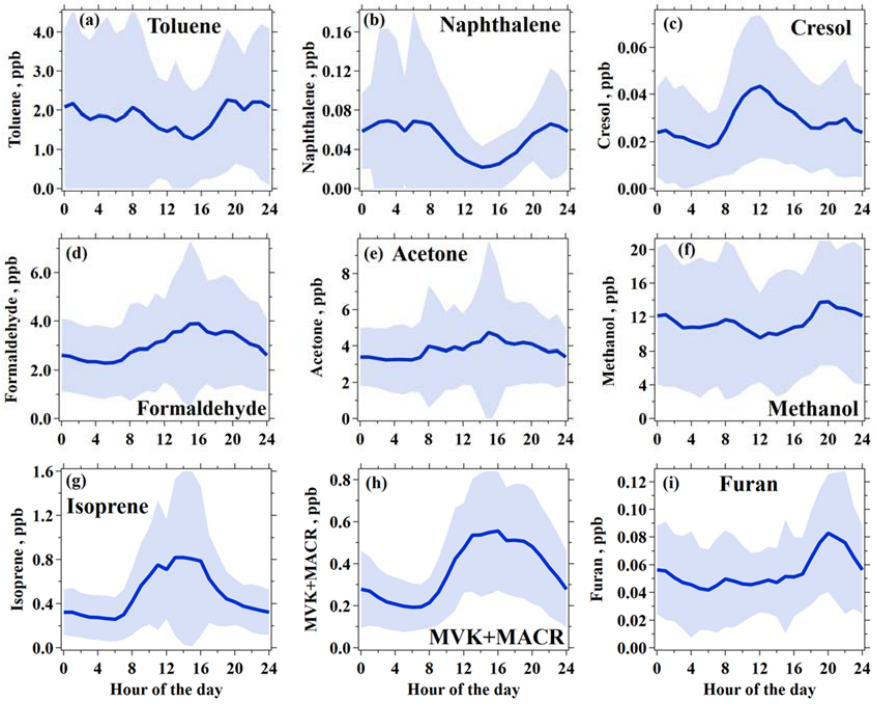

Figure 1. Diurnal variations of selected VOCs during the campaign. Blue lines and shaded areas represent averages and standard deviations, respectively.

https://doi.org/10.5194/acp-2020-152
Preprint. Discussion started: 7 May 2020

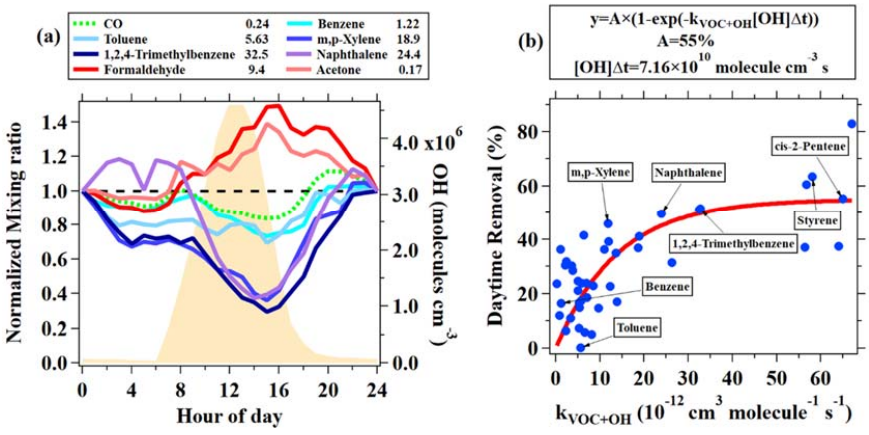

Figure 2. (a) Normalized diurnal variations of CO, five aromatic hydrocarbons (benzene, toluene, m,p-xylene, 1,2,4-trimethylbenzene and naphthalene) and two OVOCs (formaldehyde and acetone). The data are normalized to midnight values. The rate coefficients for the reactions with OH radicals are shown in the legend (in units of 10^{-12} cm^3 $molecule^{-1}$ s^{-1}). The orange shaded area indicates the average diurnal variation of simulated OH by an observation-constrained box model. (b) Daytime removal fractions of hydrocarbons as a function of their rate constants with OH. The daytime removal fractions for VOCs species were calculated from the concentration ratio between measurement at 14:00 and at 6:00-8:00.

https://doi.org/10.5194/acp-2020-152
Preprint. Discussion started: 7 May 2020

Atmospheric Chemistry and Physics Discussions

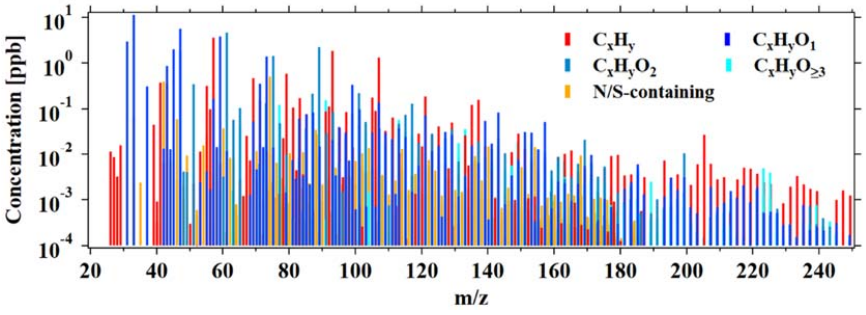

819

820 **Figure 3**. Average mass spectra obtained by PTR-ToF-MS from ambient measurement

821 during the campaign. The different ion categories are detailedly discussed in the text.

https://doi.org/10.5194/acp-2020-152
Preprint. Discussion started: 7 May 2020

Atmospheric Chemistry and Physics Discussions

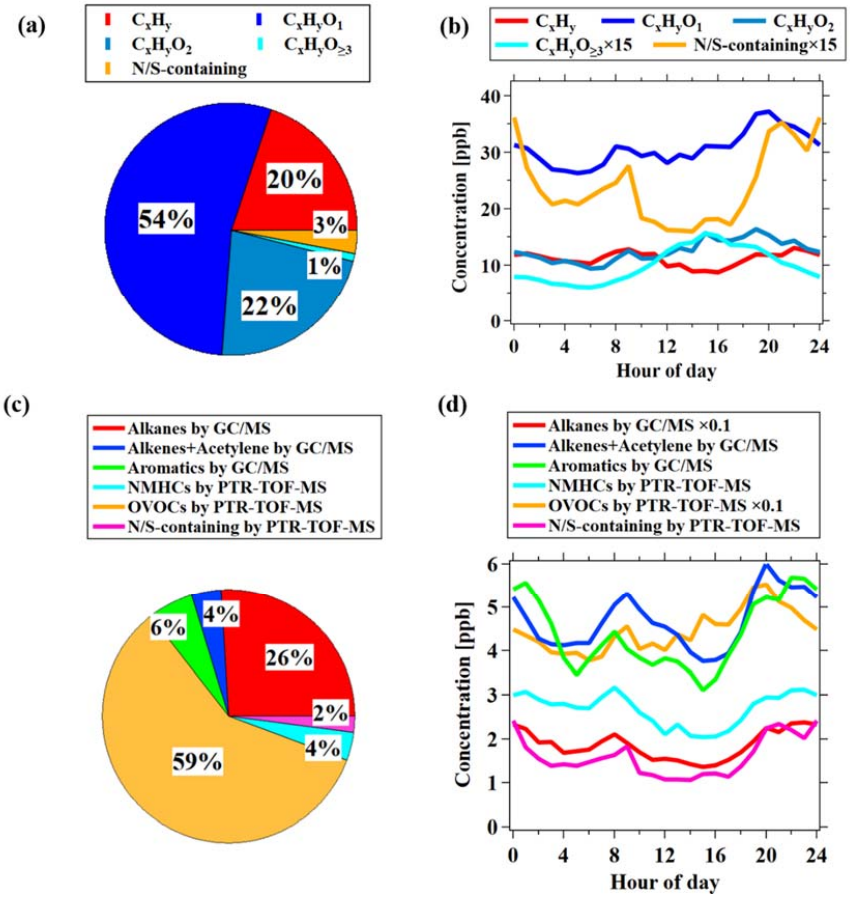

Figure 4. (a) The average concentration percentage of each category measured by PTR-ToF-MS during the campaign. The different ion categories shown in (a) and (b) are detailedly discussed in the text. (b) Diurnal variations of each category measured by PTR-ToF-MS during the campaign. (c) The average concentration percentage of each category VOCs during the observation period. Alkanes, alkenes+acetylene and aromatics were measured by GC-MS/FID, while OVOCs, N/S-containing species were measured by PTR-ToF-MS. "NMHCs measured by PTR-ToF-MS" represent hydrocarbons measured by PTR-ToF-MS after removing overlapping species with GC-MS/FID (e.g. C6-C9 aromatics, isoprene). (d) Diurnal variations of each category of VOCs shown in (c) during the campaign.

https://doi.org/10.5194/acp-2020-152
Preprint. Discussion started: 7 May 2020

Atmospheric Chemistry and Physics Discussions

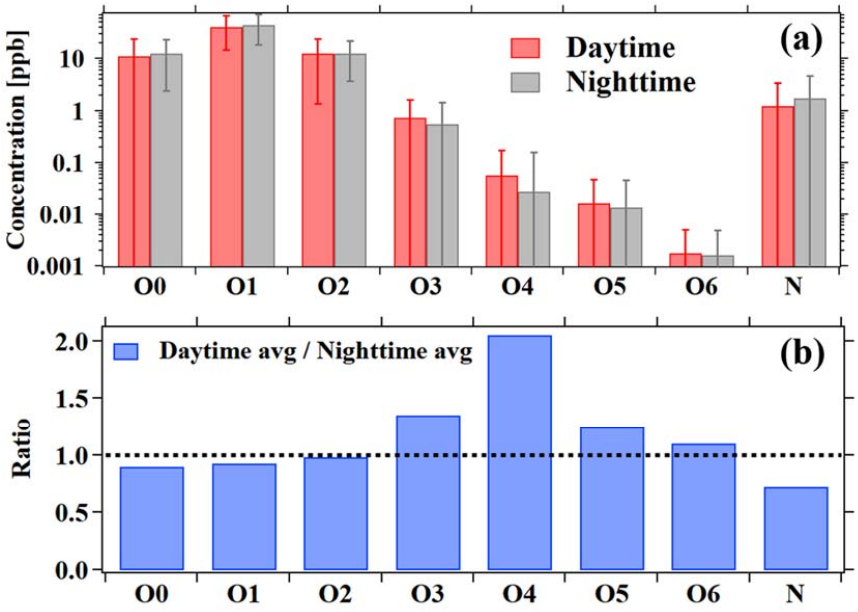

833

834 **Figure 5**. Average mixing ratios for the different groups of ions measured by PTR-ToF-
835 MS. Nighttime (18:00–6:00) averages are shown in black and daytime (6:00–18:00)
836 averages in red with the error bars indicating the standard deviations. The ratios
837 between daytime and nighttime averages are shown in the lower panel in blue.

https://doi.org/10.5194/acp-2020-152
Preprint. Discussion started: 7 May 2020

Atmospheric Chemistry and Physics Discussions

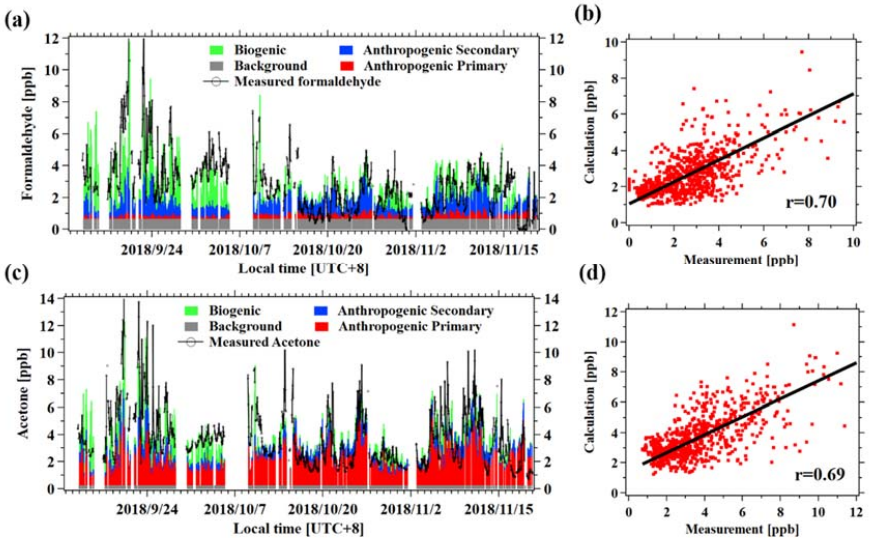

Figure 6. (a) Time series of the measured and fitted concentrations of formaldehyde from different sources. The different colors represent the four different terms of Eq. 1. (b) Scatterplot of the calculated versus the measured formaldehyde concentrations. (c) Time series of the measured and fitted concentrations of acetone from different sources. (d) Scatterplot of the calculated versus the measured acetone concentrations.

https://doi.org/10.5194/acp-2020-152
Preprint. Discussion started: 7 May 2020

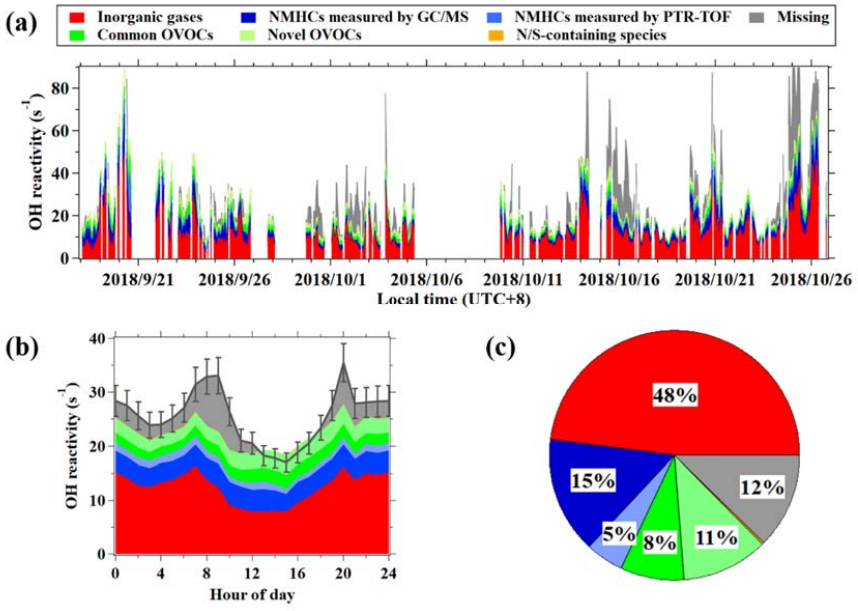

Figure 7 (a) Time series of calculated and measured OH reactivity during the campaign. (b) Diurnal variation of hourly average results of the calculated reactivity and measured OH reactivity. (c). Composition of calculated OH reactivity during the campaign.

https://doi.org/10.5194/acp-2020-152
Preprint. Discussion started: 7 May 2020

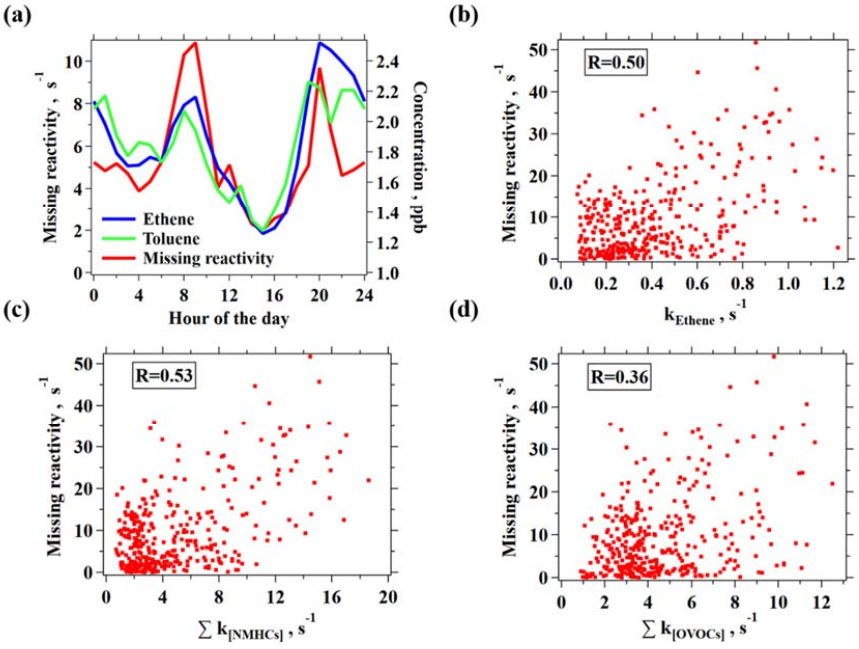

850

851 **Figure 8** (a) Diurnal variation of hourly average for missing reactivity and ethene
852 concentration. (b-d) Correlation plots of the missing reactivity versus the reactivity of
853 ethene (b), NMHCs measured by GC-MS/FID and PTR-ToF-MS (c) and OVOCs
854 measured by PTR-ToF-MS, including common OVOCs and novel OVOCs (d).